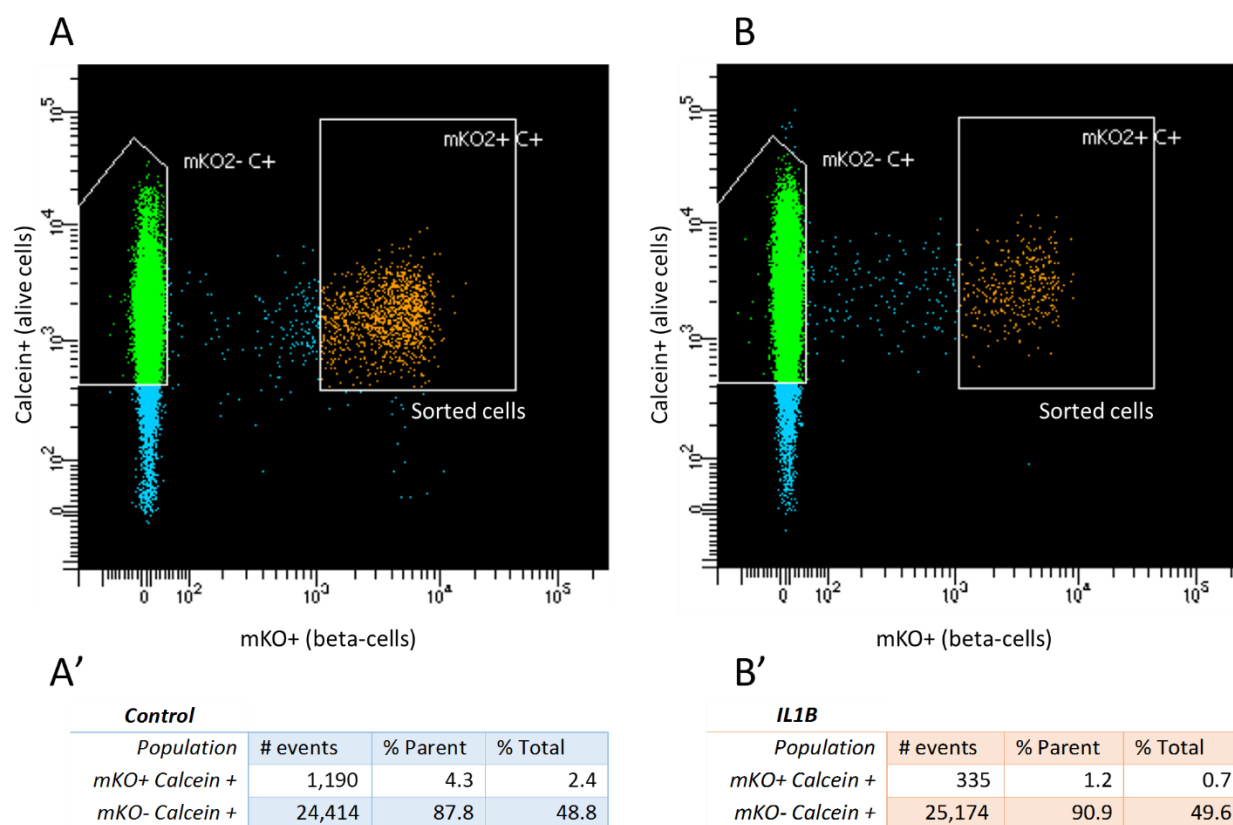


**Figure S1. Leukocytes express *tnfa* in *Tg(ins:il1b)* larvae.**

**(A-A')** Confocal slices (single plane) showing the primary islets of 3 dpf WT (A) and *Tg(ins:il1b)* larvae (A') in the background of a *Tg(tnfa:GFP)* transcriptional reporter. The arrow in A' shows an L-plastin-positive cell (magenta), which is also positive for *tnfa:GFP* (green). This cell is embedded in the islet. Some GFP-positive cells can be observed in the region corresponding to the extra-pancreatic duct in both WT and *Tg(ins:il1b)* larvae. These cells are L-plastin-negative. **(B-C)** Quantification of the proportion of GFP-positive cells among the L-plastin-positive cells in contact with the islet at 3 (B), unpaired two-tailed t-test with Welch's correction, \*p-value  $\leq 0.05$ , mean $\pm$ SD and 5 dpf (C), unpaired two-tailed t-test with Welch's correction, \*\*\*p-value  $\leq 0.001$ , mean $\pm$ SD. **(D-E)** Quantification of the total number of L-plastin cells in contact with the islet at 3 (D), unpaired two-tailed t-test with Welch's correction, \*p-value  $\leq 0.05$ , mean $\pm$ SD and 5 dpf (E), unpaired two-tailed t-test with Welch's correction, \*\*\*p-value  $\leq 0.001$ , mean $\pm$ SD. Scale bars in A-A' = 10  $\mu$ m.



**Figure S2. Fluorescence-activated cell sorting (FACS) of beta-cells.**

(A-B) Representative plots showing the sorting of beta-cells from WT (A) and *Tg(ins:il1b)* (B) fish at 3 mpf. To mark beta-cells specifically, the *Tg(ins:nlsRenilla-mKO2)* reporter line was used, which expresses nuclear Kusabira-Orange under the insulin promoter.

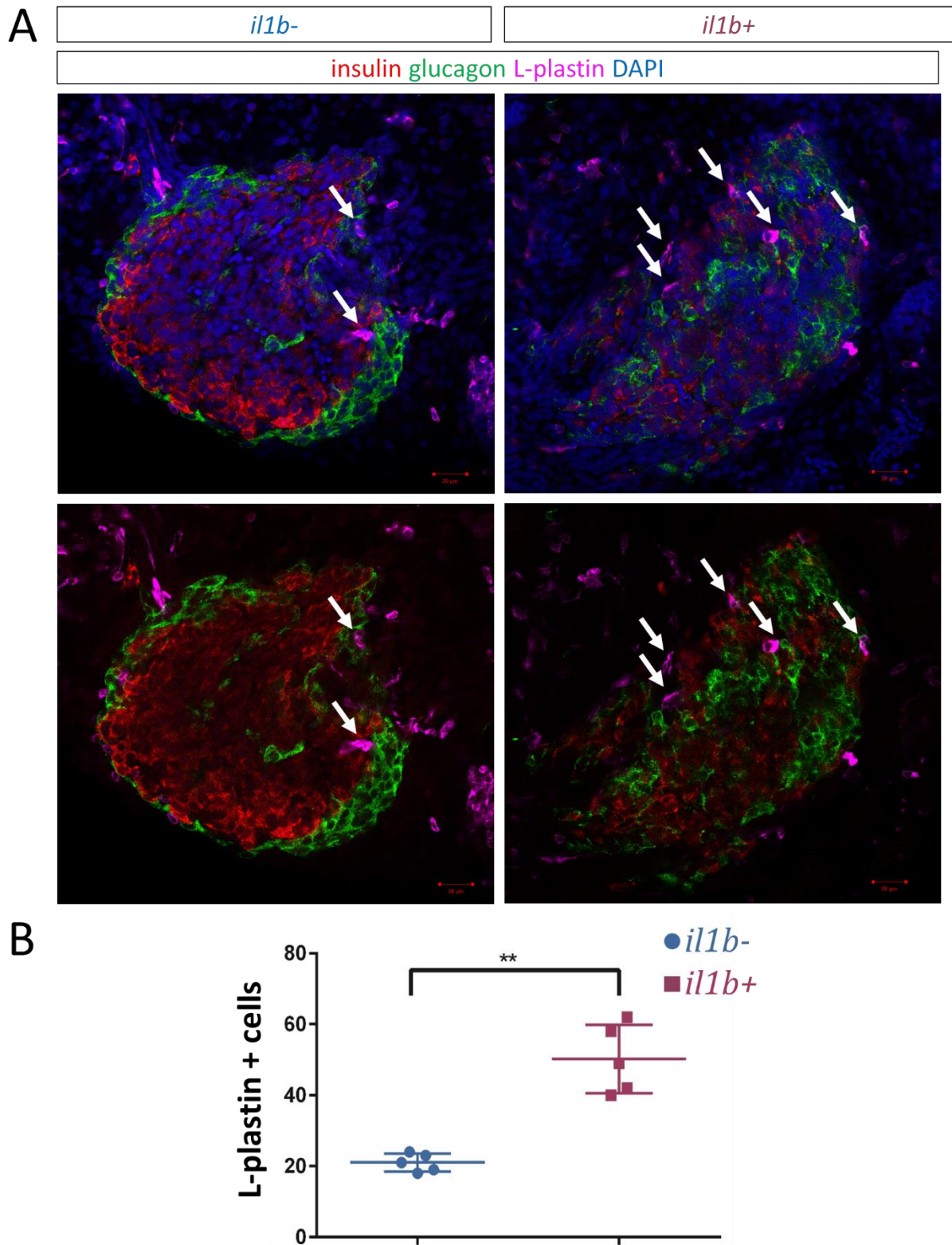


**Figure S3. Persistent increase in immune cells within the islets of *Tg(ins:il1b)* fish at 30 dpf.**

**(A)** Confocal slices (single plane) showing the primary islets in 30 dpf WT and *Tg(ins:il1b)* juveniles. Arrows point to L-plastin-positive cells. **(B)** Quantification of the number of L-plastin-positive cells per islet. *Tg(ins:il1b)* animals exhibit an increase in L-plastin-positive cells. Unpaired two-tailed t-test with Welch's correction. \*\*p-value ≤ 0.01, mean ± SD. Scale bars = 20 μm.

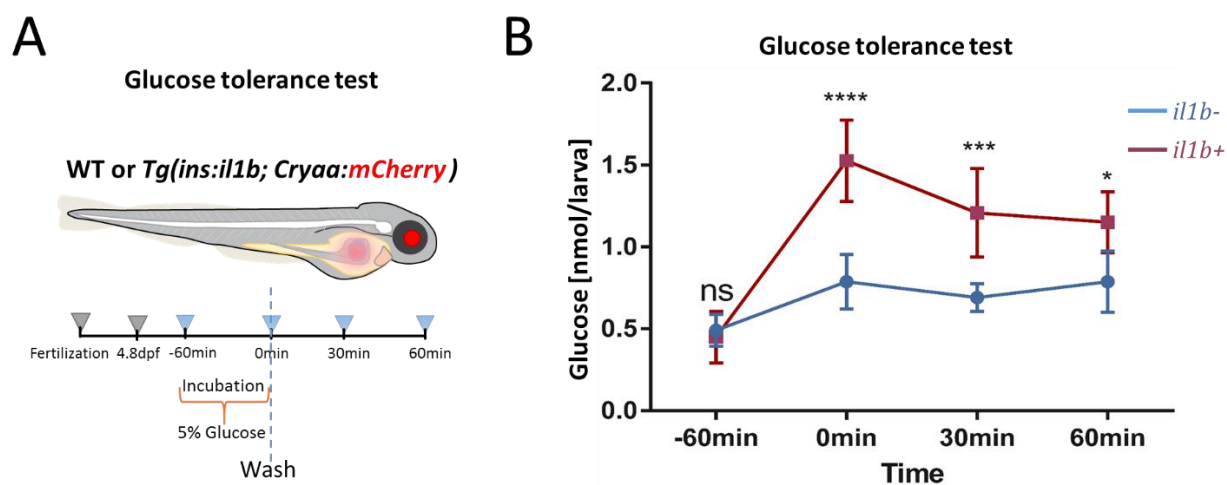


### Figure S4. Impaired glucose tolerance in *Tg(ins:il1b)* larvae

**(A)** Schematic of the glucose-tolerance test. 4.8 dpf larvae were treated for 1h in 5% glucose. The glucose was washed away by rinsing the larvae several time and the larvae were placed in egg water (E3). Samples were collected before the glucose incubation (-60 min), and following the glucose stimulation (at 0, 30 and 60 min). **(B)** Graph showing the glucose levels in WT and *Tg(ins:il1b)* larvae at each time point from two independent experiments pooled together. Each data point represents a group of 10 larvae with  $n \geq 6$  samples. Two way ANOVA with Sidak's multiple comparison test; ns: not significant, \*\*\*\* $p$ -value  $\leq 0.0001$ , \*\*\* $p$ -value  $\leq 0.001$ , \* $p$ -value  $\leq 0.05$ ; mean  $\pm$  SD.

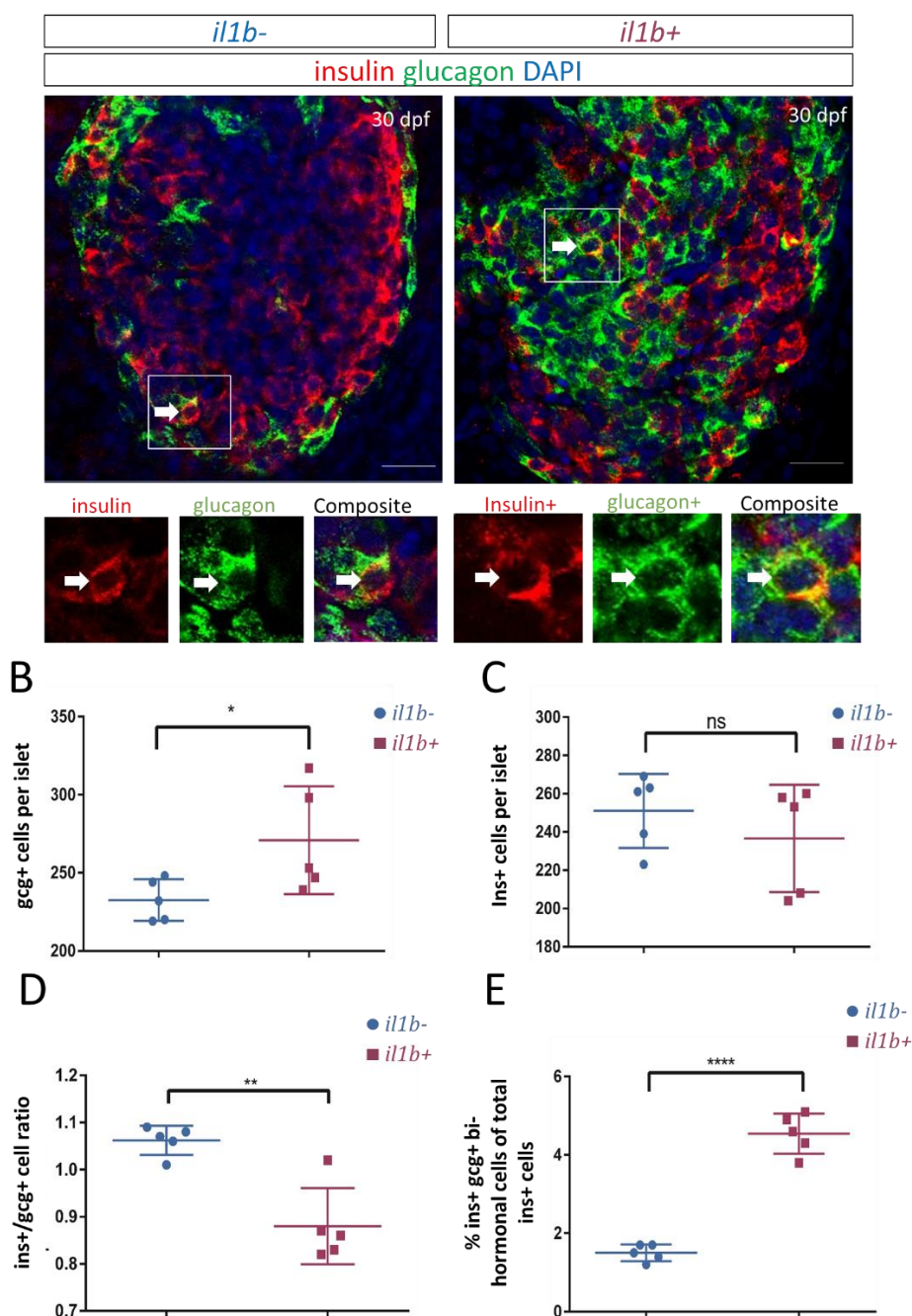


**Figure S5. *Tg(ins:il1b)* juveniles exhibit an increase in alpha-cells and higher proportion of insulin-positive cells that co-express glucagon.** (A) Confocal slices (single plane) showing the primary islets in 30 dpf WT and *Tg(ins:il1b)* juveniles. The higher-magnification insets show insulin/glucagon double-positive cells corresponding to the outlined region in the top panels (arrows). (B) Quantification of the number of glucagon-positive cells per islet. *Tg(ins:il1b)* animals exhibit an increase in glucagon-positive cells. Unpaired two-tailed t-test with Welch's correction; \*p-value  $\leq 0.05$ , mean $\pm$ SD. (C) Quantification of the number of insulin-positive cells per islet. Unpaired two-tailed t-test with Welch's correction, ns: not significant. mean $\pm$ SD. (D) Quantification of the ratio of insulin-to-glucagon-positive cells per islet. Unpaired two-tailed t-test with Welch's correction; \*\*p-value  $\leq 0.01$ , mean $\pm$ SD. (E) Quantification of portion of insulin positive cells per that co-express glucagon over the total number of insulin-positive cells per islet. Unpaired two-tailed t-test with Welch's correction; \*\*\*\*p-value  $\leq 0.0001$ , mean $\pm$ SD. Scale bars in A = 20  $\mu$ m.

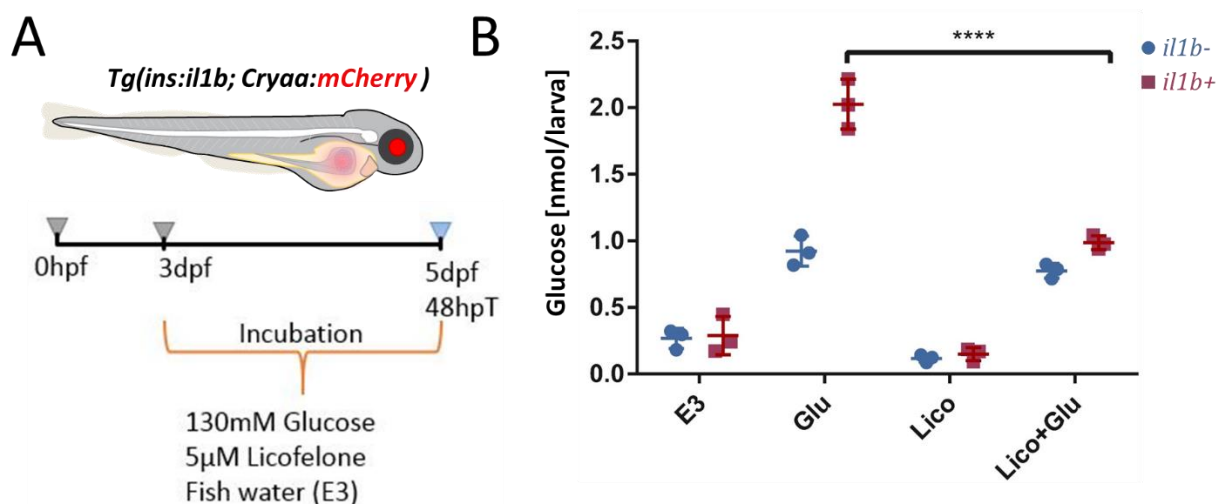


**Figure S6. The 5-LOX inhibitor Licofelone ameliorates the hyperglycemia in *Tg(ins:il1b)* larvae.**

**(A)** Schematic of the experimental setup. Larvae were treated with 5µM Licofelone or DMSO during a glucose challenge from 3-5 dpf. Glucose was measured at 5 dpf. **(B)** Plot showing average glucose values [nmol/larvae] following the treatment. The *Tg(ins:il1b)* fish showed similar values as WT in normal fish water (E3). Upon glucose challenge, the *Tg(ins:il1b)* fish showed hyperglycemia. Licofelone-treatment ameliorated the hyperglycemia in the *Tg(ins:il1b)* larvae following the glucose-challenge. In all cases, 1% DMSO was used as a vehicle control. Two way ANOVA with Sidak's multiple comparison test; \*\*\*\*p-value ≤ 0.0001. Each data point represents a pool of 10 larvae, mean±SD.

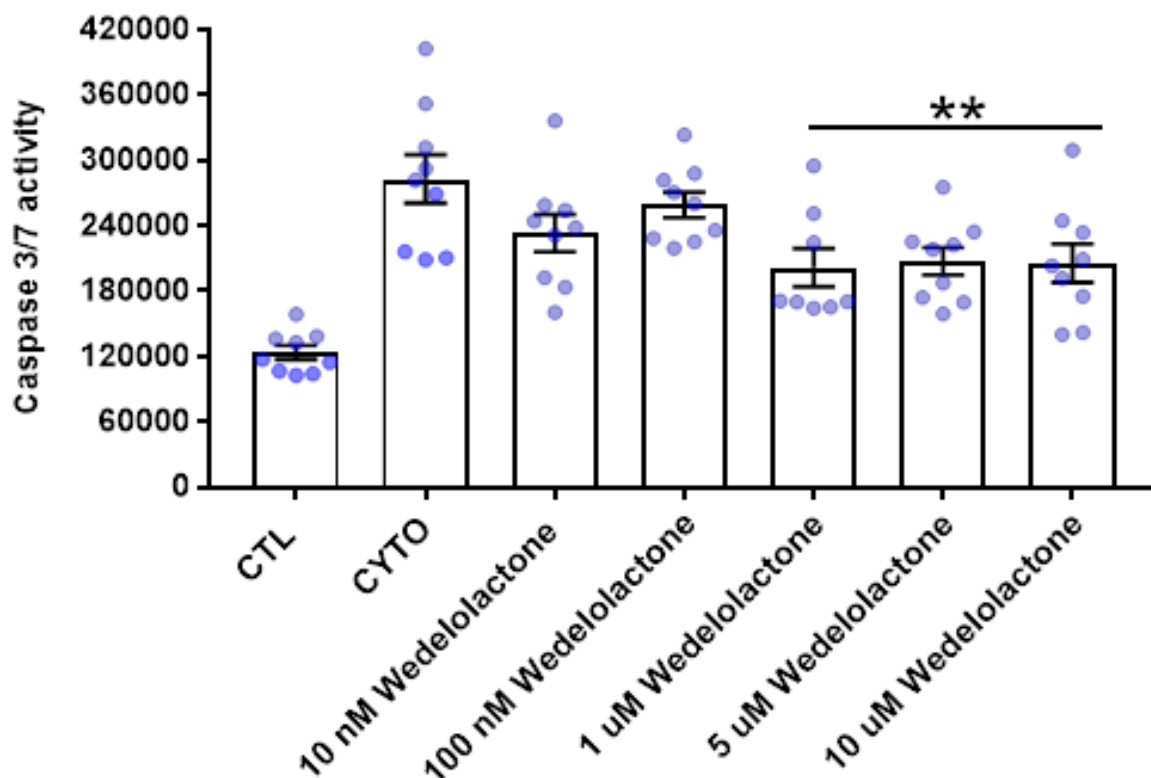
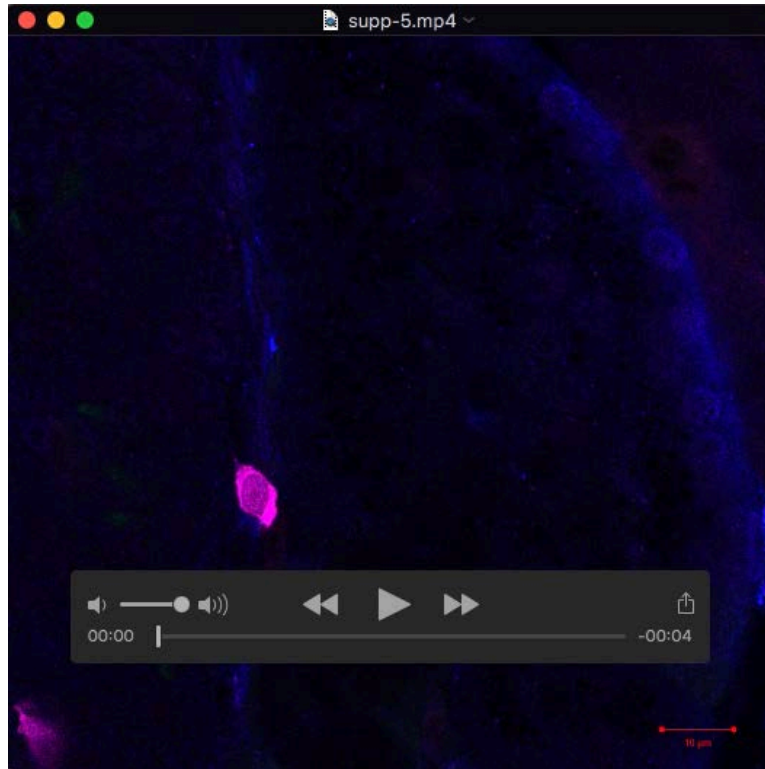
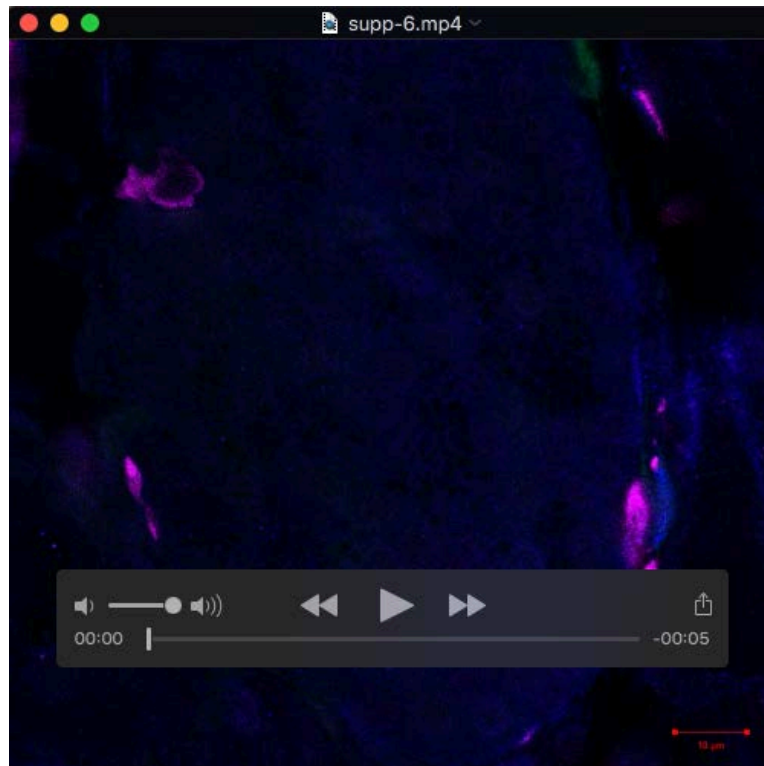


**Figure S7. Wedelolactone inhibits cytokine-induced islet-cell apoptosis without pre-treatment.**

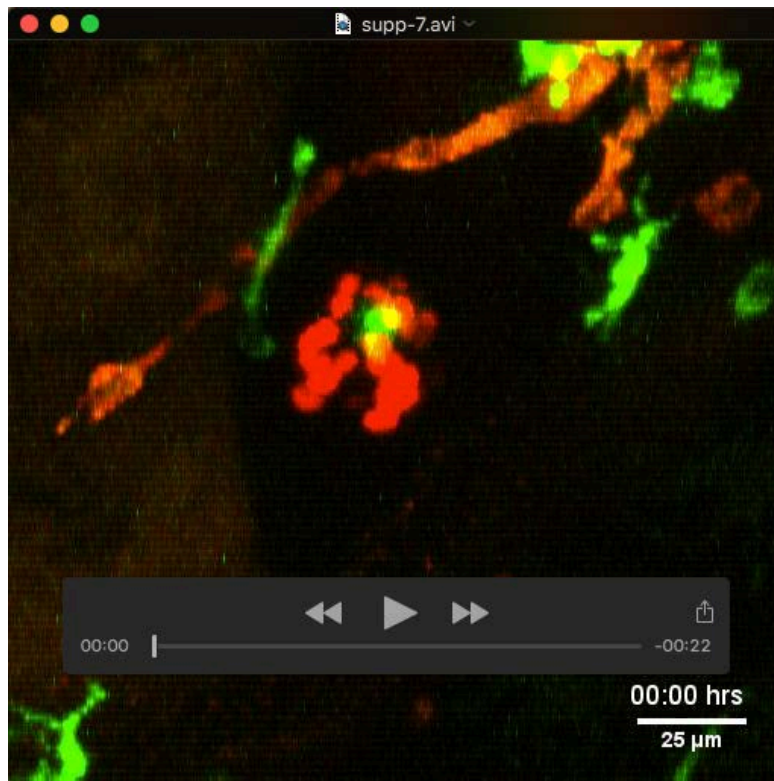
Mouse islets were incubated with increasing concentrations of Wedelolactone (10nM-10 μM), in the presence of a cytokine cocktail for 20 hours. Apoptosis was assessed by Caspase 3/7 activity. n = 9 biological replicates per treatment group. \*\*p≤0.01 by one way Anova with Dunnett's post hoc analysis.



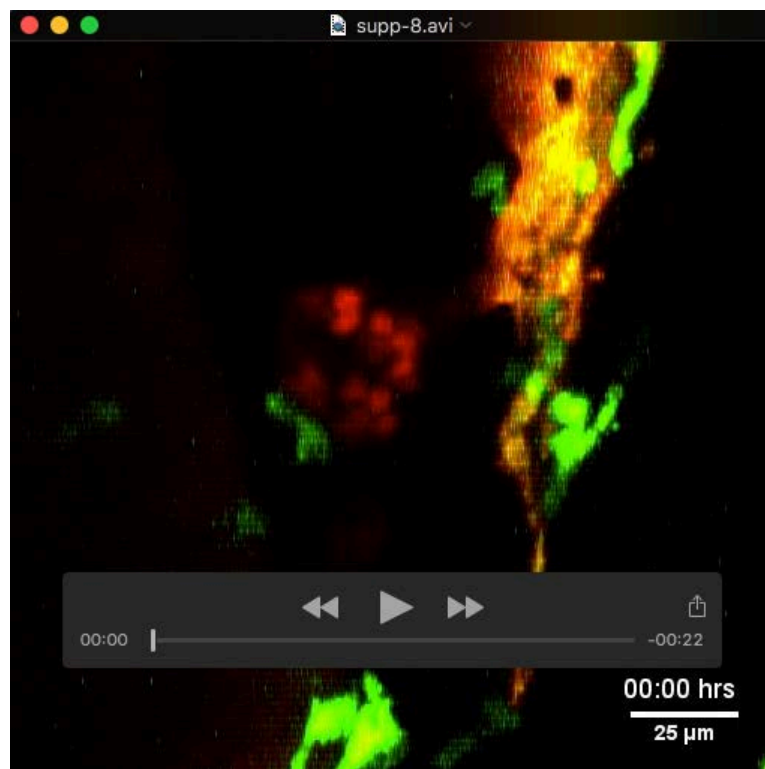
**Movie 1.** A confocal stack showing beta-cells (blue), Nf-kB activity (green) and L-plastin-positive cells in WT larvae.



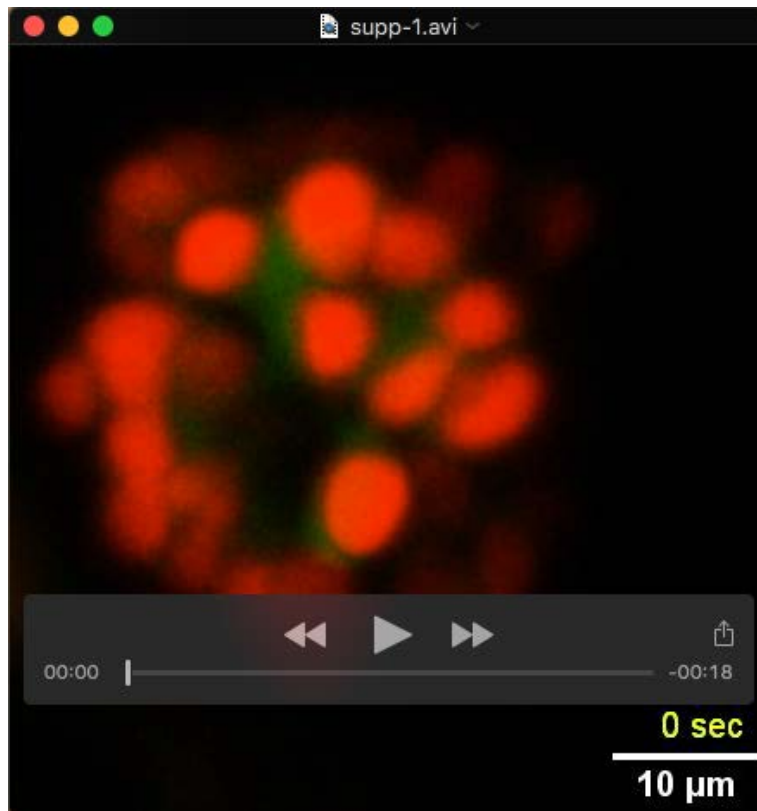
**Movie 2.** A confocal stack showing beta-cells (blue), Nf-kB activity (green) and L-plastin-positive cells in *Tg(ins:ll1b)* larvae.



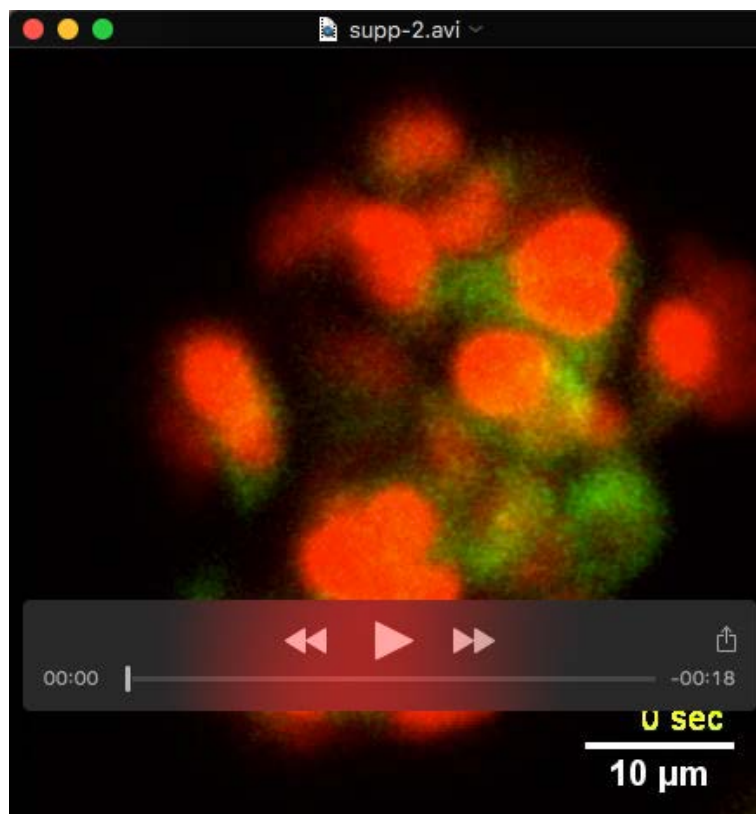
**Movie 3.** *In vivo* live imaging of macrophages (green) and beta-cells (red) in control larvae.



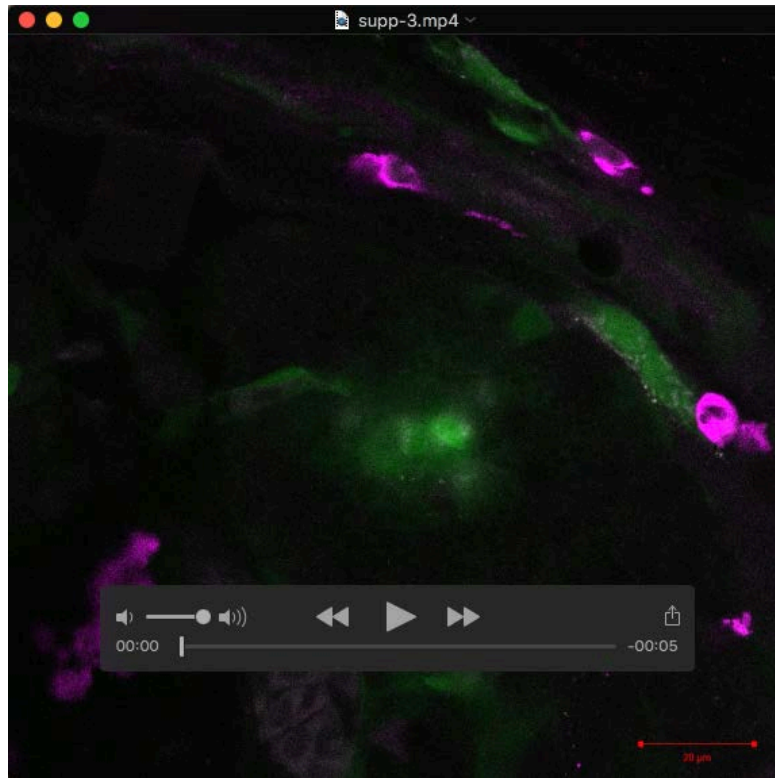
**Movie 4.** *In vivo* live imaging of macrophages (green) and beta-cells (red) in *Tg(ins:ll1b)* larvae.



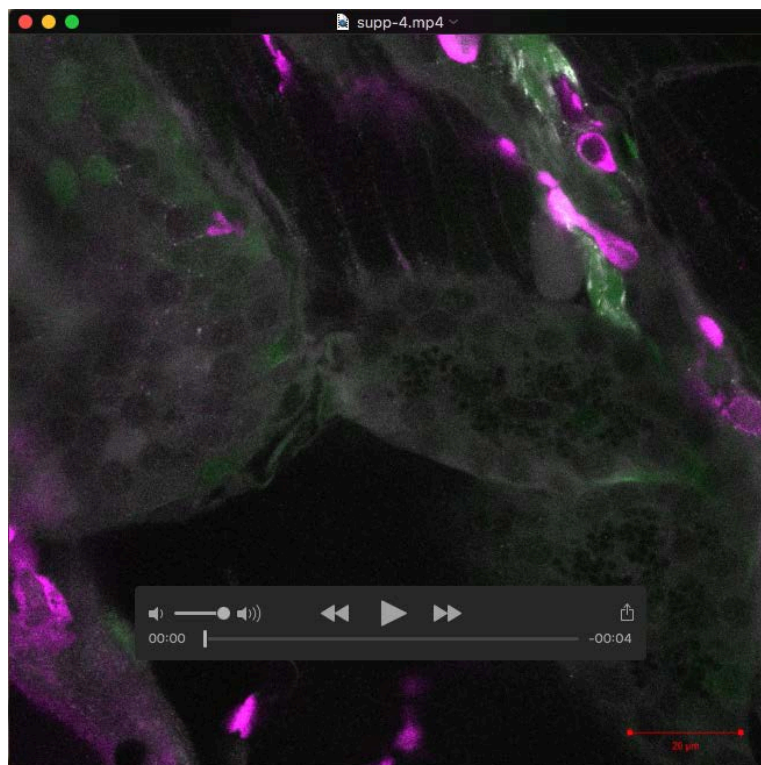
**Movie 5.** *In vivo* live imaging of glucose-stimulated calcium influx in beta-cells in control larvae



**Movie 6.** *In vivo* live imaging of glucose-stimulated calcium influx in beta-cells in *Tg(ins:Il1b)* larvae.



**Movie 7.** A confocal stack showing beta-cells (white), Nf-kB activity (green) and L-plastin-positive cells (magenta) in *Tg(ins:Il1b)* larvae treated with DMSO.



**Movie 8.** A confocal stack showing beta-cells (white), Nf-kB activity (green) and L-plastin-positive cells (magenta) in *Tg(ins:Il1b)* larvae treated with Wedelolactone.